JOURNAL OF THERMOPHYSICS AND HEAT TRANSFER
Vol. 18, No. 4, October–December 2004

Loop Heat Pipe for Spacecraft Thermal Control, Part 1: Vacuum Chamber Tests

Michelle L. Parker* and Bruce L. Drolen†
Boeing Satellite Systems, El Segundo, California 90245
and
Portonovo S. Ayyaswamy‡
University of Pennsylvania, Philadelphia, Pennsylvania 19104-6315

Detailed results of two ground-based tests to determine the thermal characteristics of loop heat pipes (LHP) with a view for application in spacecraft thermal control are presented. The tests were carried out in a thermal vacuum chamber. The first test involved one LHP and a deployable radiator, whereas the second test employed two LHPs and a deployable radiator. The data gathered from the thermal vacuum chamber tests have revealed the importance of correctly sizing the compensation chamber and fluid fill volume. The study has demonstrated the feasibility of a two LHP/deployable radiator system. The system responses to sudden large power decreases have been documented. The interaction between the two LHPs, the effects of the compensation chamber environment on performance, the effect of liquid return line routing on the radiator, and the effect of liquid return line heating are discussed. A key finding is the impact of heat leaks. The data presented show the effects of zone-to-zone heat leaks and indicate that the LHP condensers could have significant impact on each other. The data also show that an LHP condenser can have significant effects on itself where cold portions of the condenser lines have been located in the vicinity of hot portions, essentially reducing the amount of subcooling and raising the operating temperature of the LHP.

Nomenclature

g	=	gravity
Kn	=	Knudsen number
L	=	length, m
p	=	pressure (Pa)
T	=	temperature (°C, K)
T_{comp}	=	compensation chamber temperature
T_{evap}	=	evaporator temperature
T_{sat}	=	saturation temperature
T_{sink}	=	sink temperature
t	=	time
Δp	=	pressure drop
ε	=	emissivity
λ	=	mean free path

Subscripts

cap	=	capillary
cc	=	compensation chamber
cond	=	condenser
g	=	gravity
l	=	liquid
sat	=	saturated
tot	=	total
v	=	vapor
w	=	wick

Received 7 July 2003; revision received 26 March 2004; accepted for publication 27 March 2004.

*Scientist, Department of Thermophysics.
†Senior Scientist, Department of Thermophysics.
‡Professor, Department of Mechanical Engineering and Applied Mechanics (corresponding author).

Introduction

WE have carried out extensive ground-based and outer space testing to understand and predict loop heat pipe (LHP) behavior with a view for application in spacecraft thermal control.[1] The ground-based tests include two performed in a thermal vacuum chamber and two more under ambient conditions. In this paper, we present results and discussions of the ground-based vacuum chamber tests. The results of tests carried out in ambient conditions are presented in Part 2.[2] We have also numerically modeled the vacuum chamber test, and this is described in Part 3.[3] The space-based tests were conducted onboard the space shuttle STS-87, and the results are reported in Part 4.[4] We first provide a general introduction, and this is followed by a specific introduction to the problems investigated.

LHP

The heat transfer community is always in search of devices that will transport large amounts of heat over long distances with minimal temperature drops. Spacecraft thermal control systems in particular have a need for devices capable of transporting large quantities of heat, upward of 1000 W, long distances (several meters), with a low ensuing temperature drop. A low temperature difference across the device, from heat input section to heat rejection section, is important because it can impact the efficiency, size, and weight of spacecraft radiators that accept heat from the device and, in turn, reject it to space. Small temperature differentials within a heat transport device allow the radiators to run at warmer temperatures, thereby allowing optimization of radiator size. A device that does this by strictly passive means, that is, no external pump or engine, is ideal. For many years, this need has been realized by the conventional heat pipe[5–8] and the capillary pumped loop system.[9] The more recent LHP is a descendant of the conventional heat pipe, and it incorporates several of the advantages of both conventional heat pipe and capillary pumped loops while overcoming many of the limitations of each.[10–14] The LHP is also of use in ground-based applications such as solar collectors and computer cooling.

Some significant attributes of the conventional heat pipe are as follows: 1) It is self-contained. 2) It is passive. 3) It operates essentially isothermally. 4) It has high thermal conductance. 5) It can have multiple evaporators and condensers, and their locations along

the length of the heat pipe are interchangeable. This means that the heat pipe need not be manufactured with dedicated evaporator and condenser locations. In spite of all of these positive features, the conventional heat pipe also has some drawbacks. Some significant disadvantages of conventional heat pipes are as follows: 1) There are orientation and/or length limitations: Conventional heat pipes are adversely affected by operation with the evaporator above the condenser in a gravity environment because they can not generate sufficient capillary pumping force to overcome the gravity head present in this orientation. Although the capillary pumping force could be increased with a smaller pore size, this limits the length of the heat pipe because the liquid flow pressure losses through the wick associated with the smaller pore size rapidly become a factor affecting heat transport capacity. The smaller pore size would increase the pressure drop experienced by the liquid as it flowed back through the capillary structure toward the evaporator. 2) Entrainment is a problem: A direct interface exists between the vapor phase and the liquid phase as they move in opposite directions. The resulting shear forces create the possibility of liquid being removed from the capillary structure and becoming entrapped in the vapor flow. This may cause a depletion of liquid in the grooves, resulting in abrupt dryout of the evaporator. 3) There is positioning inflexibility: The heat pipe is essentially one long extrusion. It is made of metal and is quite rigid. Though the pipe can be bent to a certain degree, it is limited. The rigidity of the heat pipe and its inability to overcome significant adverse elevation makes positioning of the pipe rather constrained. It would be advantageous to have a flexible pipe, or flexible sections, and more freedom in positioning the evaporator and condenser with respect to one another. Flexible heat pipes have been made, but are still subject to some of the other drawbacks.

In the LHP, drawback 1 is overcome by using wicks with sufficiently small pore size to enable generation of the capillary pressure necessary to overcome adverse elevations, for example, evaporator above condenser, in normal (unit) gravity operation. These small pore sizes inherently lead to greater pressure drops through the wick because the pressure drop associated with flow through the wick is inversely related to pore size. However this difficulty is minimized by limiting the flow path of the liquid through the wick to just a short length in the evaporator because the pressure drop is proportional to the length. This prevents the pressure drop in the wick from being the factor limiting pore size of the wick as it is for the conventional heat pipe. Drawback 2 is overcome by separating the liquid and vapor flows. With this separation, no entrainment is possible except possibly at the surface of the wick, where high-speed vapor in the vapor grooves contacts the liquid in the wick. Finally, because the liquid and vapor transport lines are separated and flexible, and adverse elevations can be overcome, the evaporator and condenser can be placed in a variety of orientations with no detrimental impact on the heat transport capacity of the device, thus overcoming drawback 3. Thus, as can be seen in Fig. 1, the LHP forms a true loop with the working fluid exiting the evaporator as vapor, traveling through the vapor transport line, entering the condenser where heat is rejected and the fluid is condensed, and traveling through the liquid return line to a reservoir, or compensation chamber, from which the liquid enters the wick to be evaporated again.

The reservoir and the liquid it holds are key to initial start-up of the loop. Start-up refers to the initial operation of the loop when heat is first applied, evaporation begins, and circulation around the loop commences. There must be liquid present in the wick/evaporator section to have a successful start-up. Unlike a capillary pumped loop (CPL) in which the reservoir is a separate chamber where liquid is accumulated and which is actively controlled, that is heated/pressure primed, in a LHP, the reservoir is integrally connected to the evaporator. Thus, there is no need for active control to ensure the presence of liquid in the wick before start-up. The LHP relies on geometrical constraints and controlled volume of the working fluid, known as fluid charge, to ensure liquid presence in the wick for start-up. The compensation chamber and evaporator are often connected by a secondary wick to ensure liquid supply even under microgravity conditions. The sizing of the LHP and its fluid charge is such that, under design conditions, the compensation chamber can never be completely filled with liquid nor completely empty of liquid; this ensures that the wick always has a supply of liquid ready for initial start-up. This sizing scheme is an important aspect of LHPs. The charging strategy is a distinguishing factor between LHPs and CPLs. We note that CPLs are not entirely passive because they require preconditioning, but they do have the advantage of allowing placement of their reservoir remotely from the evaporator. The LHPs, on the other hand, are completely passive devices, as a standalone device no preconditioning is necessary, but their reservoirs (compensation chambers) must be located adjacent to their evaporators due to the integral nature of the two. A methodology for predicting a safe-start design envelope for a given system and loop design is discussed in Ref. 15.

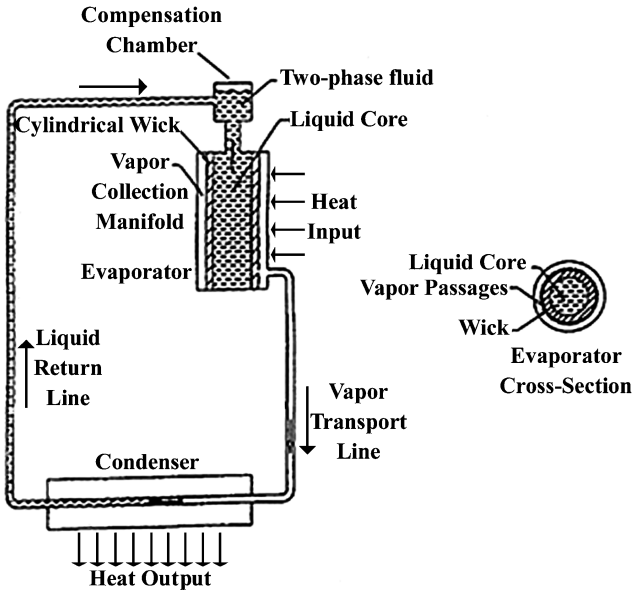

Fig. 1 Schematic of LHP.

LHP and Application in Satellite Thermal Control

The LHP's important and increasing role in satellite design make it critical to learn as much as possible about the behavior of LHPs both in unit gravity and microgravity. It is desirable to understand behavior under both conditions because, although a satellite's operational life is spent in orbit under microgravity conditions, the satellite undergoes extensive ground testing (1 g) before launch to ensure all components are working correctly. During these ground tests, electronic payloads can produce large amounts of heat and rely on the LHP to carry this heat away from the electronic units and reject it to a cool sink. Therefore, the LHPs must be able to operate successfully under unit gravity conditions.

In some spacecraft applications, multiple LHPs are integrated into a network of conventional heat pipes. The conventional heat pipes have high-power electronic units mounted to them, and they are also mounted directly to the LHP's evaporator. Heat is transferred from the electronic units, to the conventional heat pipe, and in turn to the LHP. The LHP's evaporator, compensation chamber, and transport lines are located within the spacecraft body. The transport lines are connected to flexible sections, which in turn connect to the condenser. The flexible sections allow the radiator to be stowed during launch and then deployed (unstowed) once the satellite reaches orbit. This effectively reduces the size of the satellite so that it can fit into the launch vehicle, and the radiators (termed deployable radiators) can be deployed once on station to provide the maximum amount of heat rejection area. In this context, a recent study[16] has described the design and fabrication of a propylene LHP with a flexible, deployable radiator that is intended to provide a lightweight spacecraft thermal management system. This study has also presented results of testing the LHP in an environmental chamber and in a thermal vacuum chamber. The ability to have flexible sections that allow

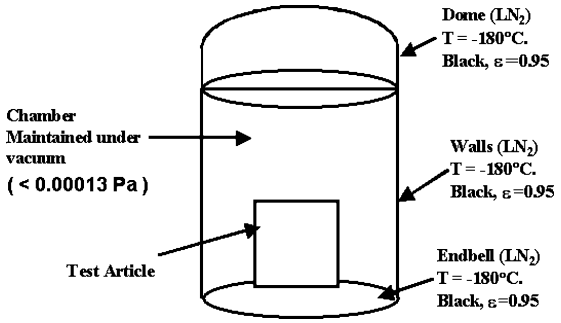

Fig. 2 Schematic of a thermal vacuum chamber.

movement, stowing, and deploying, is a crucial aspect of the LHP and to the next generation of communications satellites. No benefit would be gained from the extra radiative area if heat could not be transported to the area. The LHP enables this transport. The LHP's condenser is external to the spacecraft, mounted to the aluminum deployable radiator. It transfers its heat conductively to the radiator. The radiator's purpose is to reject the heat to a cooler sink environment. Its surface is covered with high-emittance, low-absorptivity mirrors that enhance radiation and reduce solar load while in orbit. The heat transfer occurring from the surface of the radiator while in orbit is purely radiative because no convection or conduction takes place from this external surface in the vacuum of space. The radiator rejects its heat to deep space, the ideal sink at essentially 0 K. Obviously, these conditions, 0 K and a perfect vacuum, are impossible to reproduce on Earth, but we must come as close as possible to represent accurately the thermal processes occurring, not only in the LHP, but throughout the spacecraft. To accomplish this, thermal vacuum chambers are used.[17] A schematic of the thermal vacuum chamber used in this study is shown in Fig. 2.

Vacuum Chambers for Ground-Based Simulation of Certain Aspects of Outer Space Transport

Vacuum chambers employed in our study are capable of being maintained under vacuum ($\approx 10^{-6}$ torr, 0.000133 Pa) by pumps. The temperature of the chamber can be maintained at -180°C. This is accomplished by flowing liquid nitrogen through shrouds within the walls, floor (referred to as an endbell), and ceiling (dome) of the chamber so that the surfaces of the spacecraft are rejecting heat to a sink at -180°C. The wall, endbell, and dome of the chamber are high emissivity (0.95) and black in color. They are made of steel and can withstand the force of the pressure differential between the vacuum and the ambient air pressure. The vacuum ensures that very little or no convection or conduction takes place from the external surfaces of the spacecraft to the chamber walls. This fact that little or no heat transfer, other than radiation, occurs within the chamber can be supported by a calculation of the mean free path of air, λ, at the pressure of the chamber and room temperature, and by the Knudsen number, which compares the mean free path to the characteristic length L in meters of the test article. The mean free path and the Knudsen number may be determined from

$$\lambda = 2.27 \times 10^{-5}\left(\frac{T}{p}\right) = 2.27 \times 10^{-5}\frac{298}{0.000133} = 50.9$$

$$Kn = \frac{\lambda}{L} = \frac{50.9}{2} = 25.45 \tag{1}$$

where L, the characteristic length of the test article, is 2 m. The Knudsen number in the vacuum chamber is 25.45, whereas in standard atmospheric conditions it is 3.34×10^{-10}. A Knudsen number of 1 may be considered to represent free molecular flow conditions. In our test, the Knudsen number is 25.45, which supports that little or no conduction or convection occurs within the chamber. This condition, along with the cold walls, simulates a space environment to the best of our abilities on the ground.

Role of Gravity in Ground-Based Testing of LHP

Given the abilities of the vacuum chamber to simulate the thermal environment of outer space, the only aspect we cannot recreate on the ground is the absence of gravity. For many components of a spacecraft, such as electronic units, heaters, and sensors, gravity has no impact; however, gravity does have a significant effect on heat pipes, both conventional and LHPs. As much as possible, conventional heat pipes are situated so that they operate horizontally or in reflux mode (condenser above evaporator so that gravity assists the liquid returning to the evaporator). If this is not possible, additional test heaters and/or cooling devices may be necessary to ensure continuous operation of the conventional heat pipes. LHPs can overcome adverse elevations, for example, condenser below evaporator requiring pumping of the fluid against gravity to return it to the evaporator. The LHP will operate in this orientation in 1 g, but its capability is affected. The height that the LHP can overcome is a function of the wick pore size and the pressure drops experienced in the rest of the LHP. Let Δp_{tot} denote the total pressure drop in the LHP as given by

$$\Delta p_{\text{tot}} = \Delta p_v + \Delta p_{\text{cond}} + \Delta p_\ell + \Delta p_g + \Delta p_w \tag{2}$$

where Δp_v is the pressure loss in vapor-phase transport, Δp_{cond} is the pressure drop in the two-phase portion of the condenser, Δp_ℓ is the pressure losses in the liquid-filled line, Δp_g is the pressure losses associated with gravitational head, and Δp_w is the pressure losses in the wick. For the functioning of the LHP, $\Delta p_{\text{cap}_{\max}}$ is the maximum capillary pressure that can developed for the wick and is, thus, the maximum driving potential for the LHP such that

$$\Delta p_{\text{cap}_{\max}} \geq \Delta p_{\text{tot}} \tag{3}$$

That is, the maximum capillary pressure must be equal to or greater than the sum of the pressure drops around the loop. In general, pressure drops around the loop increase with increasing input power, and so, in 1 g, the necessary inclusion of the pressure head due to gravity means the maximum input power that the LHP can handle will be reduced. For example, an LHP that can transport 600 W in microgravity may only transport 500 W in 1 g due to the portion of its capillary pumping capability that must be dedicated to overcome the gravity-induced pressure head.

Another impact of 1-g operation is the increase in operating temperatures at low input powers. At high input powers, the impact of gravity may not be noticed on operating temperatures as the gravity pressure head is less noticeable compared to other pressure drops; however, at low input powers and low mass flow rates, the gravity pressure head becomes significant compared to the others. It therefore plays the largest part in setting the temperature differential between the compensation chamber and evaporator at low flows in 1 g.

With all of these 1-g impacts identified, we reiterate that ground-based testing is required, and it is necessary to understand LHP operation on the ground as well as in space. Because of the complexity of some satellite heat pipe networks, it is not always possible to test LHPs in the preferred horizontal position. It, therefore, becomes necessary to understand the impact of gravity on LHPs in the vertical position. Operating characteristics such as temperature vs heat load, conductance of the LHP (input power vs temperature difference between the evaporator and saturation temperature), reaction to sink changes, impact of the spacecraft internal environment temperature (to which the compensation chamber, evaporator, and transport lines are exposed), and rapid power steps are important. The LHP's startup behavior is also important.

To accomplish this goal we have performed many ground-based tests including two that were performed in a thermal vacuum chamber. Two additional LHP tests were performed under ambient (standard temperature and atmospheric pressure) conditions, and they are reported in Part 2.[2] The vacuum tests were of increasing complexity; the first included just one LHP and a simulated deployable radiator, whereas the second consisted of two LHPs and a simulated deployable radiator.

We now describe the two vacuum chamber tests. Each of the tests is discussed along with data interpretation.

Test 1: One LHP and Simulated Deployable Radiator in Thermal Vacuum Chamber

This test provided experimental data on an LHP in a deployable radiator configuration. This ground-based testing was performed in January 1996 at what is now Boeing Satellite Systems, El Segundo, California in a thermal vacuum chamber to best simulate the space environment to which the LHP would be exposed when operating in orbit. The chamber was maintained under vacuum (10^{-6} torr; 1.33×10^{-4} N/m^2) throughout the duration of the test. The walls, dome, and end-bell temperatures were controlled to set the effective radiative sink temperature to which the LHP test equipment rejected heat. The lowest wall temperature achievable was approximately -180°C attained by flowing liquid nitrogen through the shrouds along the inner surfaces of the walls, dome, and endbell of the chamber.

Test Description

This test had many objectives, its overall objective being to determine how the LHP would operate as part of a system in a space simulated environment. The space environment was simulated as described earlier. To simulate the LHP being part of a system, the LHP's condenser was mounted to a simulated radiator (aluminum facesheet), which could radiate its heat to the cold walls of the chamber. Heat could be supplied to the LHP either via a conventional heat pipe mounted to the LHP's evaporator as would occur in the integration of the LHP into a satellite heat pipe network, or by heaters mounted directly to the LHP evaporator. Some more objectives of the test were 1) to demonstrate the feasibility of a deployable radiator using an LHP, 2) to determine the operating temperature as a function of power, 3) to verify LHP start-up capability, and 4) to verify the LHP's ability to handle sudden large power increases/decreases.

The hardware used for this experiment included one LHP made of stainless steel and aluminum with a Russian made sintered nickel wick and with ammonia as the working fluid, one conventional dual bore heat pipe, meaning one extrusion with two grooved vapor cavities, or bores, as shown in the cross section in Fig. 3.

The simulated deployable radiator was made of pure 1100-series aluminum with the front side painted with high emissivity ($\varepsilon = 0.85$) black primer and the backside insulated with 11-layer multilayer insulation (MLI) to reduce heat rejection from this side. The condenser of the LHP was bonded to this aluminum facesheet in a serpentine fashion. A simulated spacecraft enclosure, also made of aluminum, enclosed the evaporator, compensation chamber, and transport lines and was insulated from the cold chamber with MLI. Two radiometers were used to gauge the effective sink temperature. These radiometers were placed in front of the radiator facing the cold walls, and their temperatures were monitored. They were blanketed on the side facing the radiator and should have, in theory, run at the temperature of the effective sink to which they and the radiator were exposed. Radiometer accuracy is on the order of 20°C.

Chromalux ceramic heaters were used to supply heat to the LHP evaporator and to the dual bore heat pipe, which in turn transported the heat to the LHP evaporator. The dual bore heat pipe, is a conventional-type heat pipe with heat supplied to it via chromalux ceramic heaters at its evaporator section. Its condenser section is mounted to the evaporator of the LHP, and the heat supplied by the heaters is transported from the evaporator of the dual bore heat pipe to its condenser and then to the evaporator of the LHP. This configuration simulates that which may be present in a satellite heat pipe network, that is, conventional heat pipe supplying heat to the LHP evaporator. This setup also allowed testing of the heat transfer interface between the conventional dual bore heat pipe and the LHP evaporator, important data to have for system level design considerations. With regard to the heaters on the evaporator, they were controlled by a different heater circuit than those on the dual bore, meaning that heat could be input at these locations independent of one another. The entire test article was instrumented with 160 thermocouples, 52 on the condenser, 40 on the radiator, 3 on the liquid return line, 3 on the vapor transport line, 4 on the flex sections between the spacecraft enclosure and the deployable radiator, 3 on the compensation chamber, 6 on the evaporator, 8 on the dual bore heat pipe, 15 on the heaters supplying input power to the LHP and dual bore heat pipe, 5 on the walls of the spacecraft enclosure, and 2 on the MLI external surface. The remainder were dedicated to the radiometers and to the power harness that ran from inside the spacecraft simulator to the external chamber. This harness temperature was monitored, and blocking heaters were used in an attempt to limit the heat leak occurring through the harness. Finally, spot lamps were placed in front of the radiator to supply heat and warm the radiator, in the event of an anomalous occurrence, to prevent the ammonia in the condenser lines from freezing. These spot lamps were for contingency purposes only and, as it turned out, were not used during the test.

Figure 4 shows a schematic of the test setup. The LHP evaporator was mounted in a vertical orientation with the compensation chamber above the evaporator body. Heat was supplied to the evaporator via ceramic heaters on one side and on the other side by a 19.05-mm ($\frac{3}{4}$-in.) dual bore heat pipe operating in reflux mode, that is, condenser above evaporator so that gravity assists the return of the working fluid. The dual bore heat pipe's role was to transport heat supplied by ceramic heaters mounted to its evaporator to the evaporator of the LHP. This setup was chosen to simulate a possible heat supply method that could be used in a satellite heat pipe network. It impacted only the heat supply method, not the actual workings of the LHP. The spacecraft simulator enclosure, representing the interior of the spacecraft, surrounded the LHP evaporator, compensation chamber, and the dual bore heat pipe. The effective mass attached to LHP in this test consisted of one dual bore heat pipe and ceramic heaters, amounting to approximately 1–2 kg. No impact of this mass on the start-up of the LHP was noticeable. The test was performed in a thermal vacuum chamber as already discussed.

The environments simulated during this test included a -5°C sink temperature to simulate the time after launch when the deployable radiators are still stowed and not directly exposed to deep space, a -40°C sink to simulate the warm environment experienced during the winter season after 15 years on station, and a -180°C [liquid nitrogen (LN_2) walls] sink to simulate the cold environment experienced by the satellite during equinox at the beginning of the satellite's operational life.

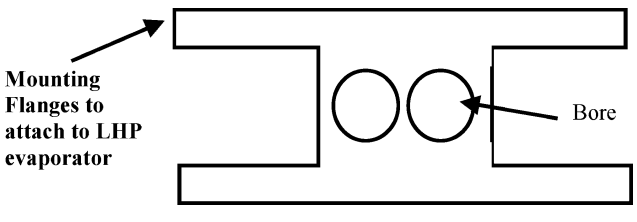

Fig. 3 DBHP schematic.

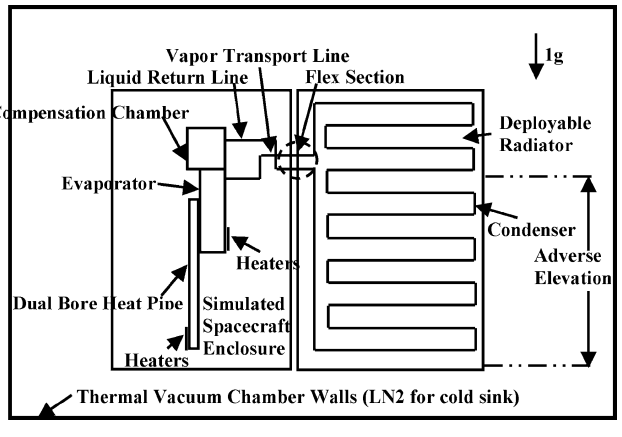

Fig. 4 February 1996 test setup.

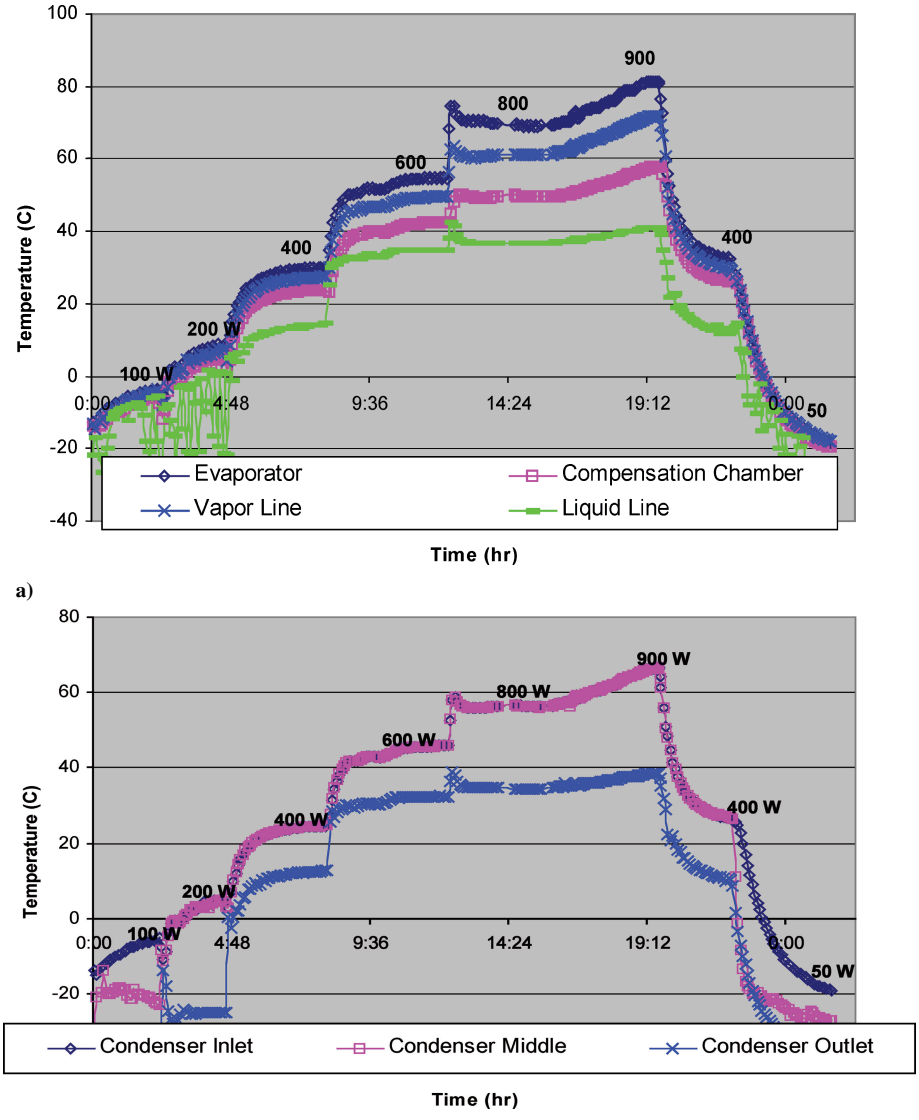

Fig. 5 Schematics of LHP warm sink operation.

Results of Test 1

A portion of the data taken during the test is shown in Figs. 5a, 5b and 6. Figure 5a shows operation of the evaporator, the compensation chamber, the vapor line, and the liquid line at warm sink (−40°C) conditions at various input power levels. Figure 5b shows the operation of the condenser (inlet, middle, and outlet) at the same conditions. Note that all power steps show smooth operation with slight cyclic behavior apparent in the liquid return line at 200 W. The LHP responds well to large power steps. Figures 6a and 6b show data from the cold sink environment (−180°C). The operation is continuous and successful; however, the cyclical behavior is again noted at 300- and 600-W input. This cyclic behavior did not disrupt operation of the LHP. Detailed discussions of temperature oscillations in LHP operation are provided by Ku et al.[18] In this test, there were indications that the compensation chamber was undersized, or that the fluid charge was too large. Portions of the condenser were blocked by liquid at high-power levels, and compensation chamber temperatures did not follow the saturation temperature at such power levels. This behavior is indicative of a liquid full compensation chamber rather than a two-phased chamber, and it is no longer able to accept excess fluid. This theory was confirmed when calculations for the sizing of the fluid fill were revisited post test and showed that too much ammonia had been introduced to the LHP for its compensation chamber size. This forced liquid into the condenser effectively shutting off, or blocking, portions of the condenser from being two-phase fluid. This condition was corrected by resizing the compensation chamber and fluid fill as discussed in the Appendix. Subsequent testing showed significant improvement. (See test 2 section to follow.) This illustrated the importance of correctly sizing the compensation chamber and fluid fill.

Figure 7 shows evaporator temperature as a function of input power for both the cold sink and the hot sink environments. The linear behavior is typical of LHPs at reasonable high power, and the repeatability of the data is demonstrated by multiple data points at a few input powers. Temperature rises as power increases to enable the LHP to reject the larger heat input over the same condenser length.

Figure 8 shows the average radiator temperature as a function of input power at the −40°C environment, along with saturation, evaporator, and dual bore temperature. Saturation temperature is measured along the first rung of the condenser. This is important system-level data because it allows conductance between the evaporator and the average radiator temperature to be calculated and subsequently used in computer simulations of the system. The conductance is a measure of the efficiency of the system. The higher is the conductance, the lower the temperature differentials through the system, and therefore, the more efficient is the system. The LHP has two definable modes of operation: a variable conductance

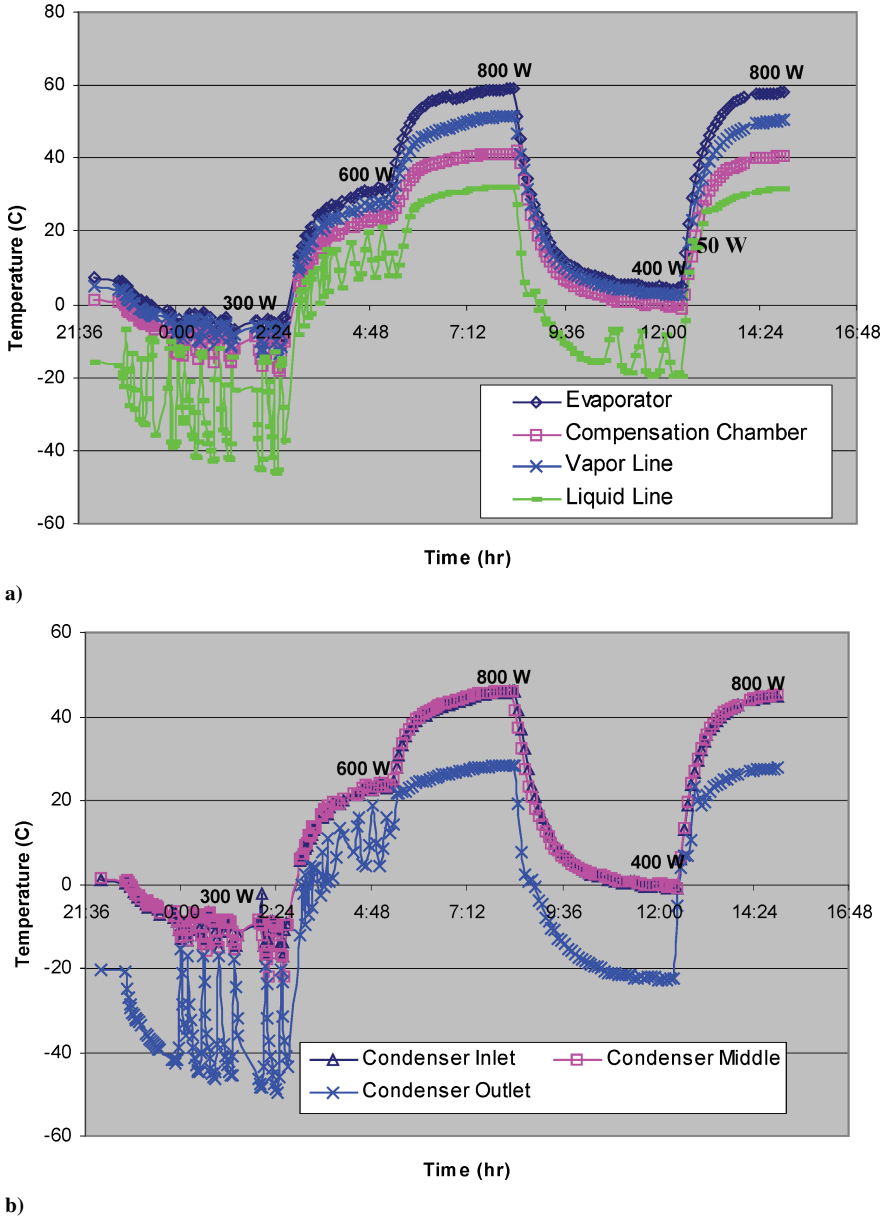

Fig. 6 LHP cold sink operation.

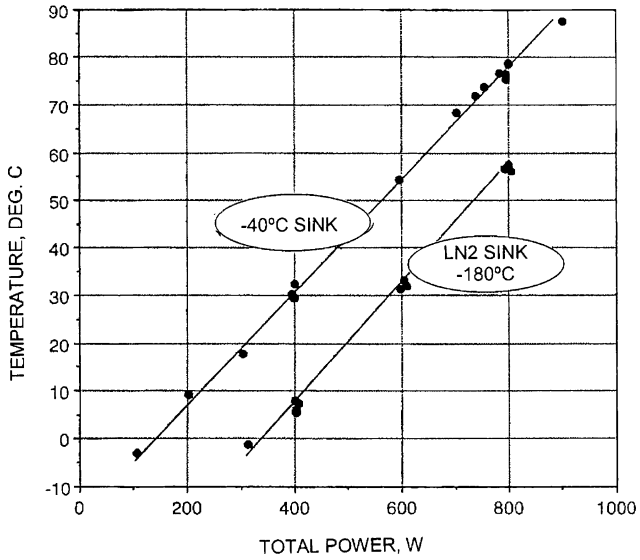

Fig. 7 LHP evaporator temperature for hot and cold sink temperature.

regime and a constant conductance regime. The variable conductance regime is characterized by the fact that the condenser is not yet fully open, that is, the liquid–vapor front lies not at the end of the condenser but somewhere near the middle. During operation in this regime, increasing power levels may be accommodated by increasing the length of the active (two-phase) portion of the condenser with relatively small, or no, increase in saturation temperature. However, once the condenser has become fully active, the only way to reject additional heat is to raise the saturation temperature of the LHP so that heat can be rejected from the same amount of area. This is the constant conductance regime where increasing power leads to proportionally increasing temperatures. The overall pressure in the LHP will also rise as the required points must remain on the saturation curve (evaporating side of the meniscus, saturated portion of the condenser, and the compensation chamber). The boundary between the variable conductance regime and the constant conductance regime varies with design and operation of the particular LHP. For the system studied here, the LHP conductance is 68 W/C.

Test 2: Two LHPs and Simulated Deployable Radiator in Thermal Vacuum Chamber

A second ground-based test was conducted in January 1997, in a large thermal vacuum chamber at what is now Boeing Satellite

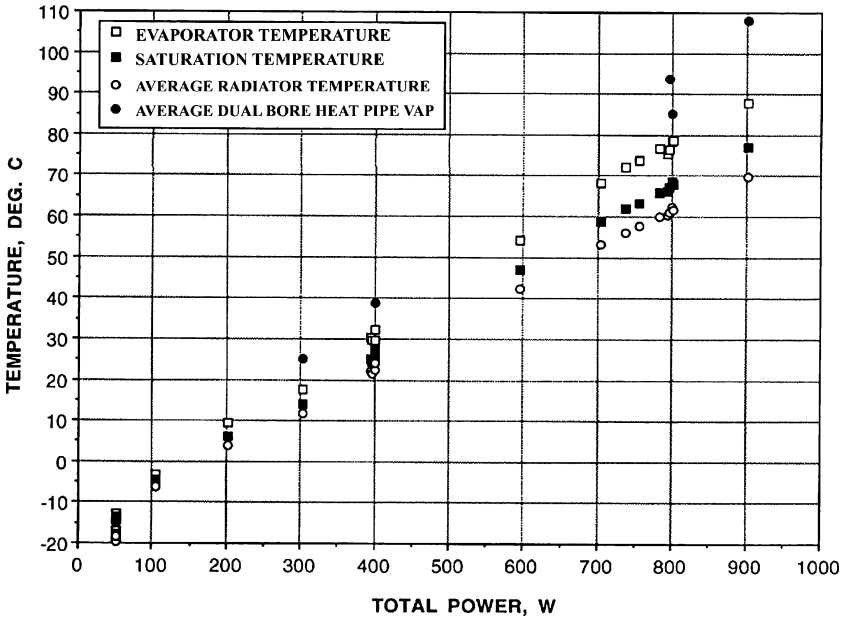

Fig. 8 Deployable radiator performance (−40°C sink).

Systems, El Segundo, California, to ascertain the performance of LHPs. Again the chamber was maintained at vacuum (10^{-6} torr; 0.00013 Pa) throughout the duration of the test, and the walls, dome, and end-bell were cooled with LN_2 to a temperature of −180°C. The primary purpose of this test was to ascertain the feasibility of a deployable radiator using two LHPs and to determine the conductive interaction present between the radiator zones of the two LHPs. Tests were performed at various power levels and at hot and cold sink temperatures. Start-ups were performed, and rapid power changes were investigated. Both LHPs performed flawlessly during all aspects of the test. One of the LHPs used for this test was the unit used in test 1 that had previously demonstrated cyclic behavior. For this LHP, a new condenser was attached, and the ammonia fill was adjusted to best fit the given compensation chamber volume. This resulted in significant performance improvement and no cyclic behavior was apparent during the duration of this test.

The specific objectives of this test were 1) to demonstrate the feasibility of a two LHP/deployable radiator system, 2) to determine the operating temperature as a function of input power, 3) to determine the system's response to sudden large power increases and decreases, 4) to determine the interaction between the two LHPs, 5) to determine the effect of the compensation chamber environment on performance, 6) to determine the effect of liquid return line routing on the radiator, and 7) to determine the effect of liquid return line heating.

Test Description

The setup for this ground test was similar to that for test 1. It consisted of the following hardware: 2 LHPs including 1 new unit (LHP1) and 1 modified unit (LHP2) from the earlier test 1, 2 dual bore heat pipes, and a simulated deployable radiator made of 1100 aluminum with the frontside painted with high emissivity ($\varepsilon = 0.85$) black primer and the backside insulated with 11-layer MLI to prevent heat rejection from the backside. A simulated spacecraft enclosure made of aluminum surrounded the evaporators, compensation chambers, transport lines, and dual bore heat pipes. This enclosure was insulated from the cold chamber using 10-layer MLI on all of its surfaces and around the dual bore heat pipes. A 10-layer blanket also separated the 2 LHP evaporator zones within the enclosure. Two radiometers were placed in front of the radiator facing the cold chamber walls to gauge effective sink temperatures as discussed for test 1. Chromalox ceramic heaters were used for heat input to the LHPs. This test was instrumented with 180 thermocouples: 32 on the LHP1 condenser, 15 on the LHP1 radiator zone, 3 on the LHP1

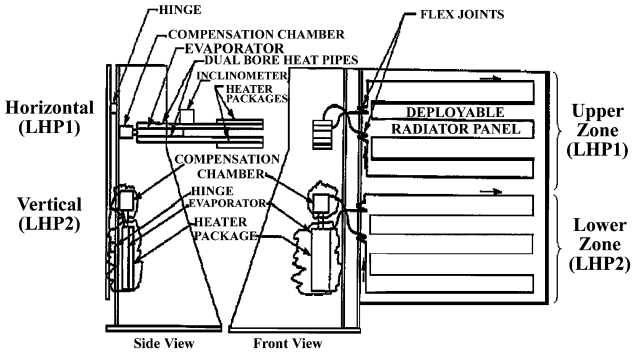

Fig. 9 Schematic of February 1997 test setup.

evaporator, 5 on the LHP1 compensation chamber, 2 on the LHP1 vapor line, 1 on the LHP1 liquid line, 18 on the LHP1 dual bore heat pipes, 12 on the LHP1 heaters, 22 on the LHP2 condenser, 9 on the LHP2 radiator, 3 on the LHP2 evaporator, 6 on the LHP2 compensation chamber, 2 on the LHP2 vapor line, 1 on the LHP2 liquid line, 6 on the LHP2 heaters, 8 on the spacecraft enclosure simulator, 4 at the midzone of the radiator between the LHP1 and LHP2, and 2 on the exterior surface of the MLI. The remainder of the thermocouples were dedicated to the radiometers and to power harness that ran from inside the spacecraft simulator to the external chamber. This harness temperature was monitored, and blocking heaters were used in an attempt to limit the heat leak occurring through the harness. Finally Calrod arrays were used to set the effective sink temperature of the radiators. The Calrod arrays are large, long, cylindrical electrical heating elements that are controlled by adjusting the voltage supplied to the arrays. They are placed in front of the radiator, and their power is varied to set effective sink temperatures that are read from the radiometers. Temperature and power data were measured every 5 min and recorded using an automated data acquisition system.

The two LHP evaporators were located within the spacecraft enclosure along with the compensation chambers, transport lines, and dual bore heat pipes. The condensers were mounted in a serpentine fashion to the deployable radiator. The condensers were mounted one above the other to create two distinct zones, the upper (LHP1) and the lower (LHP2) (Fig. 9).

The two dual bore heat pipes (DBHP) were mounted to the evaporator flanges of LHP1, one on the upper flange, and one on the

lower flange. The DBHPs delivered heat to LHP1. Heat was supplied to the DBHPs via Chromalox heaters that were installed on the far end of their length. The heaters for each DBHP were controlled by separate circuits so that it was possible to input heat to the upper DBHP, lower DBHP, or both DBHPs at the same time. A third heater circuit supplied heat to the LHP2 evaporator via Chromalox heaters placed directly on the LHP2 evaporator flanges. Therefore, there were three heater circuits that could be controlled separately: two heater circuits mounted on DBHPs servicing LHP1 and a third heater circuit mounted directly onto the evaporator of LHP2 and servicing LHP2. The LHP1 evaporator was mounted in a horizontal orientation, whereas the LHP2 evaporator was positioned vertically with the compensation chamber above the evaporator. In the LHP1 evaporator, the flow was not assisted by gravity because the compensation chamber and evaporator were at the same height. This configuration simulated some aspects of outer space conditions in the flow between these two components; however, 1-g effects, such as overcoming the gravity head from the lowest portion of the condenser back to the compensation chamber, were present. The LHP2 evaporator operated in reflux mode with the compensation chamber above the evaporator. In this test, the effective mass attached to LHP1 included two DBHPs and heater plates amounting to approximately 3–4 kg. LHP2 had only Kapton strip heaters of negligible weight attached. There was no significant difference noted between the start-ups of these two LHPs with different mass. However, it has been observed that when significant mass is attached to the LHP, the thermal capacity of the attached mass can influence the start-up characteristics. Start-up can be harder to attain when a large mass is attached to the LHP because some energy may be consumed in heating the attached mass rather than being transferred to the LHP. Figure 10 is a photograph taken of the test equipment before being sealed in the thermal vacuum chamber.

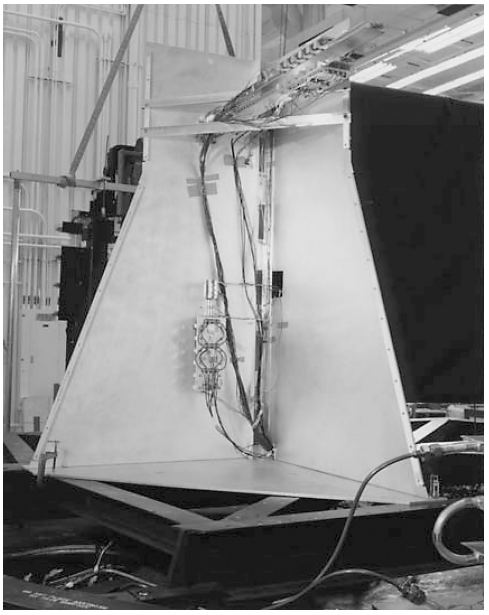

Fig. 10 Inside simulated spacecraft enclosure (LHP1 and LHP2).

The LHPs used small diameter tubing in the transport sections (vapor line, liquid line, and condenser) with L/D for the vapor line, condenser, and liquid line of 400, 3100, and 590, respectively.

A major objective of this test was to determine interactions occurring by conduction through the radiator between the two LHPs and between lines of the same LHP. The upper and lower zones on the radiator were not isolated from each other, and therefore, conduction could occur between the two zones through the aluminum radiator facesheet. The direction of this heat transfer would obviously depend on which of the LHPs was operating at a warmer temperature and the amount of subcooling present. Another important interaction that took place on the radiator was that between the liquid return line and condenser of the same LHP. In the test setup, the liquid return line runs in close proximity to the condenser bends. This was identified as a prime location for parasitic heat leaks to occur, that is, heat from the warm condenser bends conducting to the cooler liquid return line and reducing the amount of subcooling. This could have a significant impact on the operating temperature of the loop, because a reduction in subcooling (essentially increasing the temperature of the fluid returning to the compensation chamber) will raise the overall LHP temperature. No effort was made to isolate the condenser bends from the liquid return line for this test, but it was identified as an area to observe.

Observation of the two heat leaks just described, zone-to-zone and parasitic, was an important objective of this test because no previous testing had been performed with a two LHP/deployable radiator system. The type of system designed for this test would be needed to observe the true effects of these interactions.

Results of Test 2

Data were taken for a range of power levels and environments. Tests were performed at power input levels ranging from 50 to 900 W with various step sizes. Three different environmental sink temperatures were achieved: 20°C, representing predeployment of the radiators, −27°C, representing the warm sink experienced during winter end-of-life conditions, and −120°C, representing equinox beginning-of-life conditions. Start-up responses, rapid power step responses, rapid sink temperature variation, liquid line heating, power shed, and steady-state operation were all recorded. Different combinations of input power on each zone, for example, LHP1 high power, LHP2 low power, and vice versa, were also investigated to identify the effects of zone-to-zone interactions.

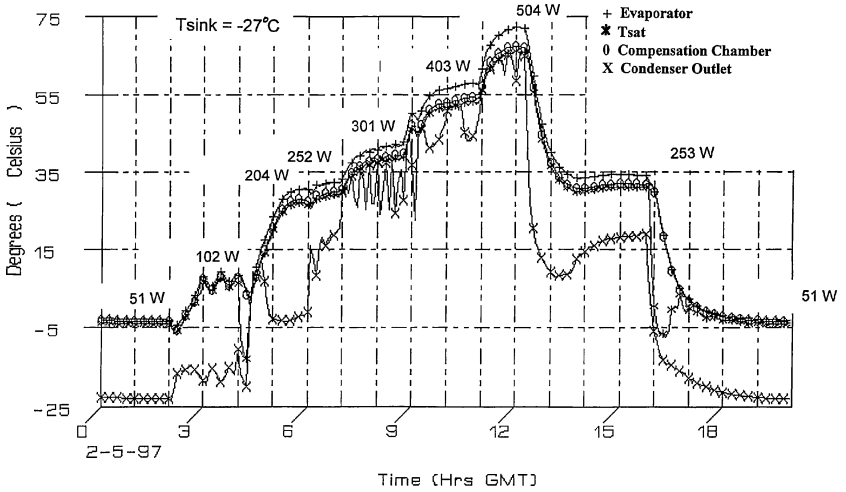

Fig. 11 Warm sink characterization, LHP1.

A portion of the data taken during the test is shown in Figs. 11–14. Figures 11 and 12 show characterization plots (temperature vs power input) taken during warm sink conditions ($T_{\text{sink}} = -27^{\circ}\text{C}$) for LHP1 and LHP2, respectively. LHP1 and LHP2 were operating simultaneously during this warm sink characterization. In both Figs. 11 and 12, moderate power steps up are taken until a maximum power input is reached and then the LHPs are subjected to large power steps down to see their reaction to such large decreases in power. Both loops operated smoothly throughout the test. The temperature dips at the condenser outlet at $t = 13$ h are due to large steps down in power. Previous to these rapid steps down, the loops were operating in full open condition, that is, condenser fully two-phase fluid. This is indicated by the condenser outlet temperature being close to the saturation temperature. Once the power down occurs, the LHP no longer needs to be fully open to reject the lower heat input. The fall in condenser

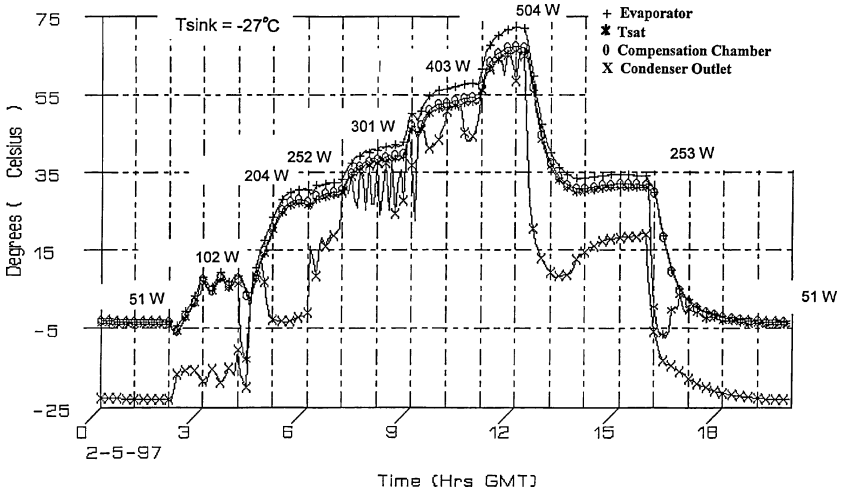

Fig. 12 Warm sink characterization, LHP2.

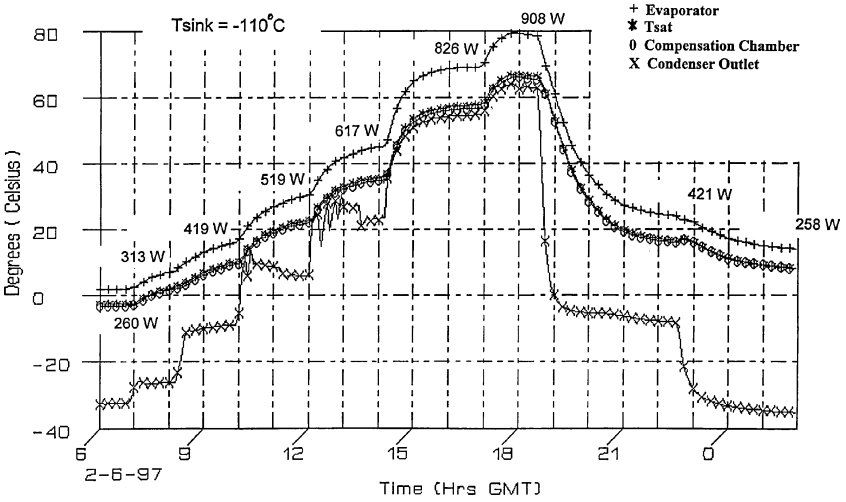

Fig. 13 Cold sink characteristics, LHP1.

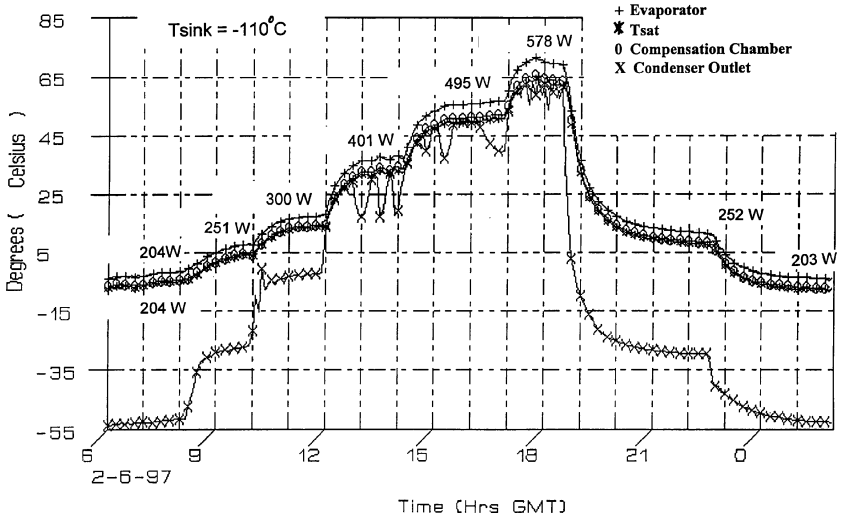

Fig. 14 Cold sink characteristics, LHP2.

outlet temperatures is a reaction to the active condenser length (two-phase portion) being decreased and the outlet position now being subcooled liquid. As the active length of the condenser is decreased in response to the power decrease, the temperature sensor at the condenser outlet location reads a subcooled liquid temperature. Essentially, the lower input heat requires a lower temperature and lesser area for rejection. The overshoot seen in Figs. 11 and 12, that is, the temperature drops and then increases, may also be explained by looking at the dropping saturation temperature. When the power step down first occurs, the saturation temperature is still high and the input power can be rejected through a small length of condenser, leaving the remainder of the condenser liquid and leading to a drop in outlet temperature. Once the saturation temperature also drops, more active length is required and, in some cases (Fig. 11), a return to the fully open condition but at a lower overall operating (saturation) temperature.

Figures 13 and 14 show characterizations of the LHPs taken during cold sink conditions ($T_{\text{sink}} = -110^{\circ}\text{C}$). Again, moderate steps up in power are taken, followed by large steps down. The loops operated smoothly and, as expected, were able to reject a larger maximum power input when radiating to colder sink before reaching 80°C, the maximum design temperature and pressure for the LHP's containment vessel.

The oscillations noted in some cases (Fig. 12 at 300 W, Fig. 13 at 617 W, and Fig. 14 at 400 W) can be attributed to the location of the temperature sensor and the location of the liquid–vapor front. In these cases, it appears that the liquid–vapor front coincides with the temperature sensor at the condenser outlet location. From this condition, even small variances in the liquid–vapor front location would be noticeable as large temperature cycles because at one point in time the reading would be the saturation temperature, whereas at the next time step it may be subcooled liquid that could be much cooler. This may be apparent when the LHP has not yet reached its steady state for a given power input: The liquid–vapor front location has not yet found its optimal spot because the saturation temperature is still changing. It is felt that some of this cycling may be present after each power step as the LHP reacts to the change; however, if the liquid–vapor interface does not exist near a temperature sensor, the behavior would not be noticeable.

Figure 15 shows the effect of zone-to-zone heat leaks. In this phase of the test, the power input of LHP1 was maintained constant at 315 W while the input power to LHP2 was increased from 200 to 600 W. A clear rise in temperature can be seen for the LHP1 components, approximately a 7°C increase, simply from the increase in heat conduction caused by raising the operating temperature of LHP2. It can be seen from the temperatures that in the first phase of the test LHP2 ran significantly cooler than LHP1, indicating a

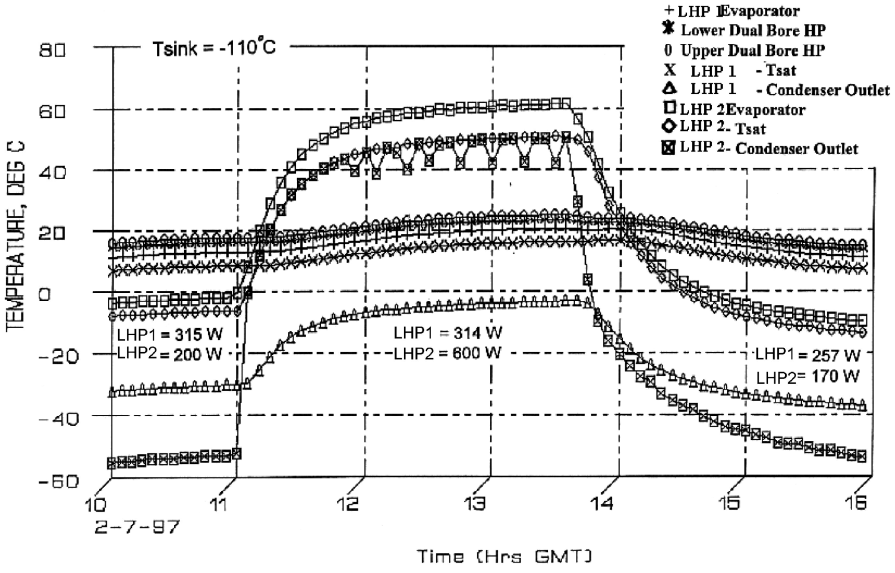

Fig. 15 Effects of LHP2 power steps on LHP1, sink.

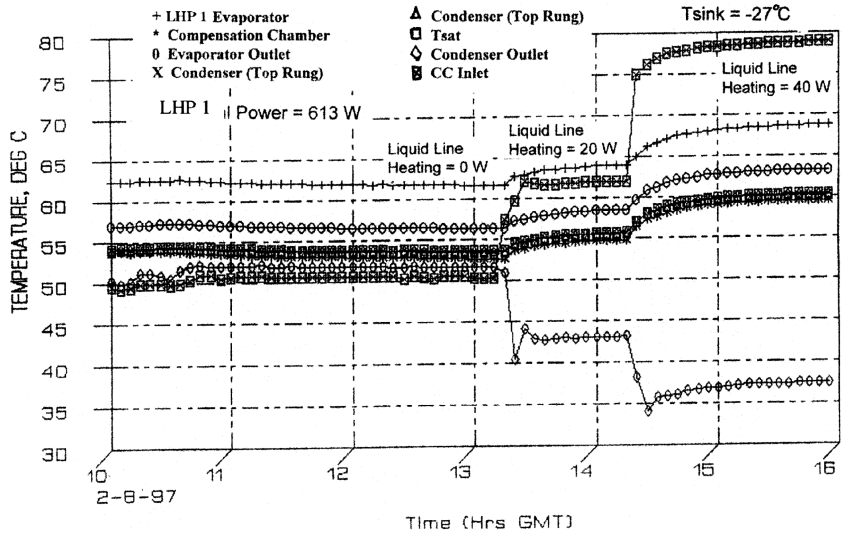

Fig. 16 LHP1 liquid return line heating: warm sink.

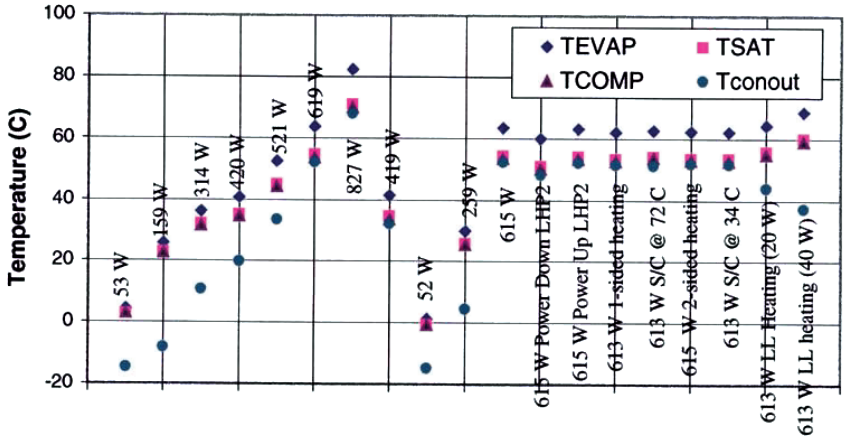

Fig. 17 LHP1 warm sink summary.

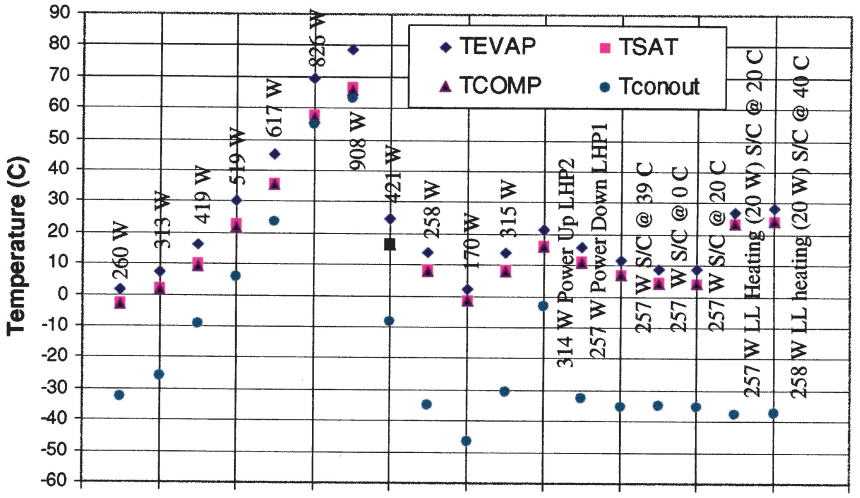

Fig. 18 LHP1 cold sink summary.

conductive heat flow from the LHP1 radiator zone to the LHP2 radiator zone. Once the LHP2 input power increased, its temperature rose above LHP1, indicating a reversal in the conductive zone-to-zone heat leak. This heat leak to the LHP1 zone results in a significant reduction in subcooling evident from the LHP1 condenser outlet temperature, which in turn causes the evident rise in operating temperature of LHP1. These data are important because they indicate clear interaction between the zones.

The impact of liquid return line heating on LHP1 is shown in Fig. 16. Clearly a small amount of heat input at the liquid return line (LRL) can have a significant effect on the operating temperature of the LHP. Again, this is caused by a reduction in the amount of subcooling present. As heat is added to the LRL, the compensation chamber and the saturation temperatures increase, resulting in a smaller zone of the radiator being required to reject the net heat load. This causes the liquid vapor front to recede up the condenser, resulting in increased subcooling and a decreased condenser outlet temperature. This in turn results in a higher operating temperature, allowing the LHP to reject the same amount of heat in a smaller length of condenser and allows more length of condenser to achieve increased subcooling. This effect is important because it is the basis for temperature control of the LHP and also can be used essentially to shut down the loop if enough heat is applied.

Figures 17 and Figure 18 show a summary of the data collected for LHP1 under warm sink (-27°C) and cold sink (-110°C) conditions, respectively. Figures 17 and 18 are interesting because they show the impact of various test conditions and also show the repeatability of the tests during similar conditions. Slight hysteresis is noticeable in Figs. 17 and 18. This phenomenon has been discussed in Ref. 19. The slight hysteresis observed in the present test is not considered detrimental to the intended application.

The experimental uncertainty in this test is 3°C based on thermocouple sensitivity and data acquisition accuracy. The scatter of data at identical test configurations was within 5°C.

Conclusions

Conclusions Based on Test 1

Test 1 verified the heat rejection capability of the system and the ability to take large power steps up and down. It allowed compilation of an operating curve (temperature vs input power) for the LHP at different sink temperatures, showed the repeatability of these data, and, finally, gave measurements of the true temperature differentials in the system. From this test the importance of correctly sizing the compensation chamber and fluid fill volume were made apparent by the presence of 1) liquid-blocked condenser legs at high power and 2) compensation chamber temperatures that did not follow the saturation temperature at high-power levels. Based on the investigation into that behavior, the compensation chamber and fluid fill were resized, and the LHP was used again in the next ground test with no repeat occurrence of the cyclic behavior.

The experimental uncertainty in this test is $\pm 3^{\circ}$C based on thermocouple sensitivity and data acquisition accuracy. The scatter of data at identical test configurations was within 4°C.

Conclusions Based on Test 2

Overall, this ground-based test provided extremely important information regarding a two LHP/deployable radiator system. It successfully met its initial objectives, including to demonstrate the feasibility of a two LHP/deployable radiator system, to determine the operating temperature as a function of input power, to determine the system's response to sudden large power decreases, to determine the interaction between the two LHPs, to determine the effects of the compensation chamber environment on performance, to determine the effect of LRL routing on the radiator, and to determine the effect of LRL heating as were shown in Figs. 16–18. A key finding was the obvious impact of heat leaks. The data from this test clearly showed the effects of zone-to-zone heat leaks and indicated that the LHP condensers could have significant impact on each other. The data also showed that an LHP condenser can have significant effects on itself, where cold portions of the condenser lines have been located in the vicinity of hot portions, essentially reducing the amount of subcooling and raising the operation temperature of the LHP.

Appendix: Charge/Fill

Sizing of the LHP is extremely important. The LHP relies solely on geometrical constraints to ensure start-up; no external means are used, for example, reservoir heaters; and this leads to the importance of appropriate sizing of the working fluid charge (volume) and the compensation chamber volume. Before sizing the compensation chamber and determining the charge, it is necessary to know the following about the particular LHP: cold operating temperature, hot operating temperature, line lengths and diameter, evaporator dimensions, and wick parameters, for example, inner and outer radii, porosity, and groove dimensions.

Two unknowns, the compensation chamber volume and the mass of charge, must be determined, and two conditions are used for this determination. The first condition is the ability to start up in the cold case when the fluid experiences the most contraction. The second is the capacity to contain the working fluid in the hot case when the fluid undergoes the most expansion.

In the first condition, the ability to start up means that there must be liquid present in the wick for evaporation when heat is applied. The cold case is used because this is when the fluid will fill the least volume. A cold operating temperature is selected based on the application and conditions to be seen by the LHP. The freezing point of the working fluid must be avoided. Once the cold temperature has been identified, the properties of the working fluid at that point can be obtained. The requirement for start up is that there must be liquid in the evaporator. This can be ensured by sizing the compensation chamber and charge such that at the coldest operating temperature there is still liquid in the compensation chamber. If liquid is present in the compensation chamber, it will be present in the evaporator due to the integral nature of the two. Therefore, it is only when the compensation chamber is empty (or close to it) that we have to worry about lack of liquid in the evaporator. Based on this worst-case position of the fluid, and knowledge of the volume of the loop except for the compensation chamber and the properties of the working fluid at the specified temperature, we can arrive at an equation in terms of the compensation chamber volume and the mass of the charge that reflects the worst-case position of the liquid and vapor in the loop at start-up:

$$m_{\text{charge}} = \rho_{\ell,\text{cold}}(\beta V_{\text{cc}} + V_{\text{pw}} + V_{\text{sw}} + V_{\text{liq line}} + V_{\text{cond}} + V_{\text{vap line}} + V_{\text{owg}}) + \rho_{v,\text{cold}}\{(1-\beta)V_{\text{cc}}\} \quad \text{(A1)}$$

where ρ is density, β is the percentage of compensation chamber that is liquid full in the cold case (user defined), V_{cc} is the volume of the compensation chamber, V_{pw} is the liquid volume of primary wick (including pores and inner wick grooves), V_{sw} is the liquid volume of secondary wick, and V_{owg} is the liquid volume of outer wick grooves.

The second condition calls for the LHP to be able to contain the volume of working fluid at the hot operating temperature when it will occupy the greatest volume. Again, with knowledge of the worst case position of fluid, the volume of the loop, the hot operating temperature, and the properties of the working fluid at this temperature, an equation can be written containing the unknowns, mass of charge, and compensation chamber volume that reflects the worst-case position of the vapor and liquid for the hottest loop operating condition:

$$m_{\text{charge}} = \rho_{\ell,\text{hot}}(\alpha V_{\text{cc}} + V_{\text{pw}} + V_{\text{sw}} + V_{\text{liq line}}) + \rho_{v,\text{hot}}[V_{\text{owg}} + (1-\alpha)V_{\text{cc}} + V_{\text{vap line}} + V_{\text{cond}}] \quad \text{(A2)}$$

where α is the percentage of compensation chamber that is liquid full in the hot case (user defined) and $(1-\alpha)$ is the space in the compensation chamber allowed for non-condensable gas storage at the end of life.

Now, with two equations with two unknowns, it is possible to solve for the unknowns. When this approach is used, the compensation chamber size and charge can be designed to ensure start-up and operating characteristics. This is a very important design step for appropriate behavior of the LHP because without correctly determining the sizing, liquid supply to the wick before start-up cannot be guaranteed, and this guarantee is a key aspect of LHP operation. Likewise, it is necessary to avoid overfill at hot conditions and full power, as seen in the first test.

Acknowledgments

The authors acknowledge Boeing Satellite Systems, formerly Hughes Space and Communications, for support of this research. The authors thank Lynda Mules for help with preparation of the manuscript.

References

[1]Parker, M. L., "Modeling of Loop Heat Pipes with Applications to Spacecraft Thermal Control," Ph.D. Dissertation, Dept. of Mechanical Engineering and Applied Mechanics, Univ. of Pennsylvania, Philadelphia, Aug. 2000.

[2]Parker, M. L., Drolen, B. L., and Ayyaswamy, P. S., "Loop Heat Pipe for Spacecraft Thermal Control, Part 2: Ambient Conditions Test," *Journal of Thermophysics and Heat Transfer* (to be published).

[3]Parker, M. L., Drolen, B. L., and Ayyaswamy, P. S., "Study of a Loop Heat Pipe for Spacecraft Thermal Control, Part 3: Numerical Simulation" (submitted for publication).

[4]Parker, M. L., Drolen, B. L., and Ayyaswamy, P. S., "Studies with a Loop Heat Pipe for Spacecraft Thermal Control, Part 4: Experiments Aboard Space Shuttle Columbia" (submitted for publication).

[5]Winter, E. R. F., and Barsch, W. O., "The Heat Pipe," *Advances in Heat Transfer*, edited by T. Irvine and J. P. Hartnett, Vol. 7, Academic Press, New York, 1971, pp. 219–320g.

[6]Ivanovskii, M. N., Sorokin, V. P., and Yagodkin, I. V., *The Physical Principles of Heat Pipe*, Clarendon, Oxford, 1982.

[7]Peterson, G. P., and Ortega, A., "Thermal Control of Electronic Equipment and Devices," *Advances in Heat Transfer*, edited by T. Irvine and J. P. Hartnett, Vol. 20, Academic Press, New York, 1990, pp. 181–314.

[8]Faghri, A., *Heat Pipe Science and Technology*, Taylor and Francis, Washington, DC, 1995.

[9]Ku, J., "Overview of Capillary Pumped Loop Technology," *Heat Pipes and Capillary Pumped Loops*, Vol. ASME HTD 236, American Society of Mechanical Engineers, Fairfield, NJ, 1993, pp. 1–17.

[10]Maidanik, Y. F., Fershtater, Y. G., and Gorchnow, K. A., 1991, "Capillary-Pump Loop for the Systems of Thermal Regulation of Spacecraft," *Proceedings of the 4th European Symposium on Space Environmental and Control Systems*, European Space Agency, ESA SP-324, 1991, p. 88.

[11]Wolf, D. A., Ernst, D. H., and Phillips, A. L., "Loop Heat Pipes—Their Performance and Potential," *24th International Conference on Environmental Systems*, SAE Transactions, Vol. 4, Society of Automotive Engineers, Warrendale, PA, 1994, pp. 1612–1618.

[12]Krotiuk, W. J., 1997, "Engineering Testing of the Capillary Pumped Loop Thermal Control System for the NASA EOS-AM Spacecraft," *Proceedings of the 32nd Intersociety Energy Conversion Engineering Conference*, Vol. 2, No. 2, AlChE Publications, New York, 1997, pp. 1463–1469.

[13]Ku, J., "Operating Characteristics of Loop Heat Pipes," 29th International Conf. on Environmental Systems, SAE Paper 1999-01-2007, 1999.

[14]Butler, D., Ku, J., and Swanson, T., "Loop Heat Pipes and Capillary Pumped Loops—An Applications Perspective," *Proceedings of the Space Technology and Applications International Forum* (STAIF-2002), edited by M. El-Genk, AIP CP 608, American Inst. of Physics, New York, 2002, pp. 49–56.

[15]Baumann, J., Cullimore, B., Yendler, B., and Buchan, E., "Noncondensible Gas, Mass, and Adverse Tilt Effects on the Start-up of Loop Heat Pipes," 29th International Conf. on Environmental Systems, SAE Paper 1999-01-2048, 1999.

[16]Krotiuk, W. J., Crowley, C. J., and J. C. Rozzi, 2002, "Propylene Loop Heat Pipe with a Lightweight, Flexible, Deployable Radiator," *Proceedings of the Space Technology and Applications International Forum* (STAIF-2002), edited by M. El-Genk, AIP CP 608, American Inst. of Physics, New York, 2002, pp. 37–48.

[17]Ottenstein, L., Ku, J., and Feenan, D., "Thermal Vacuum Testing of a Novel Loop Heat Pipe Design for the Swift BAT Instrument," *Proceedings of the Space Technology and Applications International Forum* (STAIF-2003), edited by M. El-Genk, AIP CP 654, American Inst. of Physics, New York, 2003, pp. 33–41.

[18]Ku, J., Ottenstein, L., Kobel, M., Rogers, P., and Kaya, T., "Temperature Oscillations in Loop Heat Pipe Operation," *Proceedings of the Space Technology and Applications International Forum* (STAIF-2001), edited by M. El-Genk, AIP CP 552, American Inst. of Physics, New York, 2001, pp. 255–262.

[19]Kaya, T., and Ku, J., "Investigation of the Temperature Hysteresis Phenomenon of a Loop Pipe," 33rd National Heat Transfer Conf., Paper 108, Aug. 1999.